Asian Journal of Nanoscience and Materials 3 (2020) 203-219

SPC

Journal of Medicinal and Nanomaterials Chemistry

Journal homepage: https://jmnc.samipubco.com/

Orginal Research Article

An efficient synthesis of 4,4'-(aryl methylene)-bis (1*H*-pyrazol-5-ol)s over graphene oxide Functionalized pyridine-methanesulfonate as a novel nanocatalyst

Esmael Rostami*, Zahra Kordrostami

Department of Chemistry, Payame Noor University, PO BOX 19395-3697 Tehran, Iran

ARTICLE INFORMATION

Received: 21 October 2019
Received in revised: 14 January 2020
Accepted: 14 January 2020
Available online: 25 April 2020

DOI: 10.48309/JMNC.2020.3.4

KEYWORDS

Graphene oxide
Pyridine methanesulfonate
Pyrazole
Solvent-free
Nanocatalyst
Multicomponent reaction

ABSTRACT

In this study, graphene oxide was functionalized with 3-aminopyridine to prepare a novel nanocatalyst known as the graphene oxide functionalized pyridine-methanesulfonate (GO@PyH-CH_3SO_3). The GO@PyH-CH_3SO_3 was then employed as an effective nanocatalyst to prepare 4, 4'-(aryl methylene)-bis(1H-pyrazol-5-ols) via one-pot multicomponent condensation reaction of aldehydes with 3-methyl-1-phenyl-1*H*-pyrazol-5(4*H*)-one. The best reaction condition involved the use of 0.02 g of the catalyst for 20 min and at 70 °C without using any solvent. Also, the reusability of catalyst and product yield in five runs was examined and no significant change was observed. The leaching test was utilized to assess the nature of the catalytic activity, and the results showed the heterogeneous condition for the catalytic activity. Efficiently and capability of the GO@PyH-CH_3SO_3 catalyst and other catalysts were compared and showed the superior properties of this catalyst.

Corresponding author, email: esmaelrostami@gmail.com (E. Rostami).
Tel.: +98 771 5559489.

Graphical Abstract

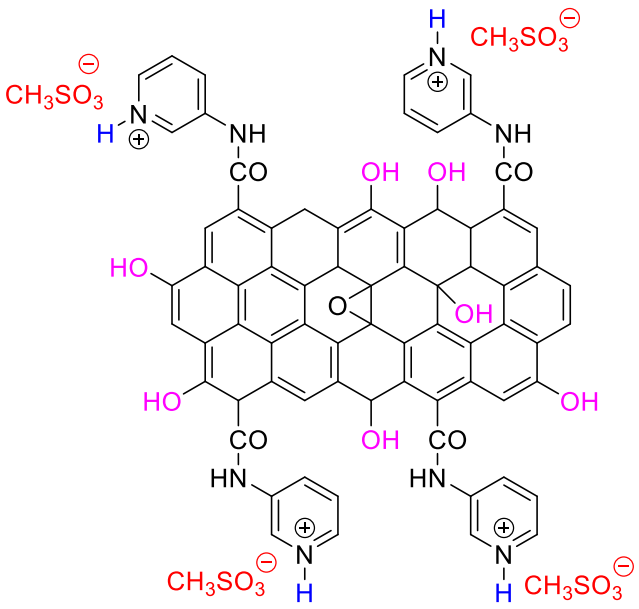

Introduction

In recent years, nanoscience has opened new horizons to investigate new systems [1]. With the help of nanocience, it is now possible to explore and use new procedures and materials. Nanotechnology has been utilized by a series of researchers in chemistry، biology، medicine، and physics. So, it can be classified as a multidisciplinary field [2]. The application of nanocatalysts in organic reaction has become a significant topic in organic synthesis [3].

Graphene is a one-layer-thick carbon allotrope with excellent properties making it an interesting substance in numerous applications [4]. This material has several unique features, including high hardness, high thermal and electrical conductivity, nontoxicity, inexpensiveness, ease of handling and preparation, thermal and acid and basic high stability and transparent [5, 6]. Graphene oxide is a graphene derivative possessing several hydroxides, ether and carboxylic acid groups [7]. In comparison with graphene, graphene oxide is more hydrophilic and its functional groups could be functionalized to optimize the new and efficient properties [8]. Its facile functionalization routes can help in designing new catalysts for the organic syntheses, especially the supported catalysts [9].

Pyrazoles with the five-member ring can occur in the structure of numerous biologically active compounds [10-12], which has made it an important bio-active drug target. This drug targets have been utilized as analgesic, anti-anxiety, anti-inflammatory and antipyretic agents [13]. Similar to pyrazole derivatives, 2, 4-Dihy dro-3H-pyrazol-3-one derivatives such as 4, 4'-(ary lmethylene)-bis (3-methyl-1-phenyl-1*H*-pyrazol-5-ols) have exhibited efficient biological properties among which antibacterial [14], gastric secretion stimulatory [15], antidepressant [16], antipyretic [17], anti-inflammatory [18], and antifilarial features can

be mentioned [19]. Other derivatives of pyrazoles, such as, 4,4'-(aryl methylene)-bis (1*H*-pyrazol-5-ols) can be used as insecticides [20], pesticides [21], and fungicides [22]. Extraction and purification of metal ions have been also carried out by 4, 4'- (aryl methylene)-bis (1*H*-pyrazol-5-ols) [23, 24].

The best route for the synthesis of 4, 4′-(arylmethylene)-bis (1*H*-pyrazol-5-ol)s is condensation of 3-methyl-1-phenyl-5-pyrazolone (2eq.) and aldehydes at the presence of catalysts. A wide range of catalysts with acidic, basic, and oxidation-reduction features can be employed for this transformation, among which, silica-bonded S-sulfonic acid [25], poly (ethyleneglycol)-bound sulfonic acid [26], silica sulfuric acid [27], ceric ammonium nitrate [28], tetramethyl-tetra-3, 4-pyridinoporphyrazinato copper(II) methyl sulfate [29], lithium hydroxide monohydrate [30], sulfuric acid ([3-(3 silicapropyl) sulfanyl]propyl) ester [31], 1, 3 disulfonic acid imidazolium tetrachloroaluminate [32], 3-aminopropylated silica gel [33], phosphomolybdic acid [34], *N*-(3-silicapropyl)-N-methyl imidazolium hydrogen sulfate [35], sodium dodecylsulfate [36], 1, 3, 5-tris (hydrogensulfato) benzene [37], 2-hydroxy ethyl-ammonium acetate [38], cellulose sulfuric acid [39] and xanthan sulfuric acid [40] can be mentioned. These procedures, however, suffer from some disadvantages including, the use of toxic solvents, harsh reaction conditions, the use of expensive and toxic catalysts, low yield, long reaction times, purification and work-up problems, deviation from the green chemistry, unwanted by-products, and requiring higher amounts of catalysts.

In this research study, a new nano-graphene oxide-based catalyst was synthesized using the 3-aminopyridine and methanesulfonic acid. The 3-aminopyridine-functionalized graphene oxide was prepared, and then resulting product was treated with methanesulfonic acid to produce the nano-catalyst. The catalyst structure was further confirmed by several analytical and spectroscopic procedures. Finally, the catalyst was employed to prepare 4, 4'-(aryl methylene)-bis (1*H*-pyrazol-5-ol)s as biologically active derivatives from the reaction of aldehydes with 3-methyl-1-phenyl-1*H*-pyrazol-5(4*H*)-one.

Experimental

Materials and methods

All the chemicals were purchased from Merck and Fluka Chemical Companies. The reactions were performed under the hood cupboard. The obtained products were identified by comparing their melting points with the reported ones. Melting points were recorded by a thermal scientific apparatus using the open capillary tubes. Thin layer chromatography (TLC) was also performed on Merck F_{254} alumina plates. ^{1}HNMR and ^{13}CNMR spectra were recorded using the Bruker Avance 400 and 500 MHz spectrometers. Thermogravimetric analysis (TGA) was conducted using an SDT Q600 V20.9 Build 20 apparatus. Fourier transform infrared (FT-IR) spectra of the samples were recorded by Bruker and Shimadzu IR-470 spectrometers using the potassium bromide pellets. The elemental concentration of the samples was evaluated using a semi-quantitative EDX (Tescan Mira III, Czech) apparatus. Scanning electron microscopy (SEM), (Tescan Mira III model, Czech) was also utilized to study the shape and surface morphology of the samples. X-ray diffractometer (PW1730) was also employed to study the X-ray diffraction (XRD) patterns using Cu-Kα radiation at 40 kV and 30 mA, and scanning rate of 1s in the 2θ range of 5-80°.

Preparation of graphene oxide functionalized 3-aminopyridine (GO@Py)

The graphene oxide was prepared from oxidizing of graphite via modified Hummer's method [41]. GO (1 g) was added to tetrahydrofuran (20 mL) and dimethyl acetamide (10 mL) solvent mixtures and sonicated using ultrasonic bath for 30 min to obtain a homogeneous emulsion. Then, 3-aminopyridine (5 mmol, 0.47 g), *N, N'*-dicyclohexylcarbodiimide (5 mmol, 1.03 g) and triethylamine (6 mmol, 0.60 g) were added at room temperature and stirring was continued for 48 h. Then, the resulting mixture was centrifuged and washed repeatedly with deionized water and ethanol through centrifugation process, and dried under an efficient vacuum at 60 °C to provide graphene oxide functionalized pyridine (GO@Py). IR (KBr) (ν_{max}/ cm^{-1}): 1024, 1628, 1726, 2924, and 3422.

Preparation of graphene oxide functionalized pyridine-methanesulfonate (GO@PyH-CH_3SO_3)

Methanesulfonic acid (8 mmol, 0.77 g) was added to sonicated (Ultrasonic bath, 30 min) GO functionalized 3-aminopyridine (GO@Py) (1 g) at room temperature in methanol (20 mL) and stirred for 24 h. After centrifugation and washing the product with ethanol through centrifugation, graphene oxide functionalized pyridine-methanesulfonate (GO@PyH-CH_3SO_3) was prepared as a black powder. IR (KBr) (ν_{max}/ cm^{-1}): 892.4, 1088.4, 1243.9, 1312, 1436.6, 1573.9, 1626.5, 2850.8, 2929.1, and 3327.2.

General procedure for synthesis of 4,4'-(aryl methylene)-bis(1H-pyrazol-5-ol)s

To arylaldehyde (1 mmol) were added 3-methyl-1-phenyl-1*H*-pyrazol-5 (4*H*)-one (2 mmol, 0.34 g) and GO@PyH-CH_3SO_3 (0.02 g) and the mixture was heated at 70 °C for an appropriate time. After completion of the reaction (monitored by TLC), ethanol (10 mL) was added to the mixture, heated and filtered. Then, by cooling to room temperature, the product was precipitated. The catalysts on the filter paper was washed with ethanol several times and dried and then was used in the reaction again. This process was repeated 4 times to examine the durability and recoverability of catalyst and reactivity in the reaction.

Selected spectral data of 4,4'-(aryl methylene)-bis (1H-pyrazol-5-ol)s

4, 4'-[(3-Nitrophenyl) methylene]-bis (3-methyl-1-phenyl-1H-pyrazol-5-ol) (3c)

^{1}H NMR (500 MHz, DMSO-d_6): δ 2.35 (6H, s), 5.15 (1H, s), 7.25 (2H, t, *J* = 7.62 Hz), 7.44 (3H, t, *J* = 7.71 Hz), 7.60 (1H, t, *J* = 8.03 Hz), 7.71 (3H, d, *J* = 7.06 Hz), 8.08 (2H, d, *J* = 13.73 Hz), 13.90 (2H, s). ^{13}C NMR (125 MHz, DMSO-d_6, δ/ppm): 12.0, 33.3, 120.9, 121.1, 121.2, 121.6, 122.22, 126.2, 129.4, 130.1, 134.8, 145.0, 146.7, 148.2.

4,4'-[(4-Chlorophenyl) methylene]-bis (3-methyl-1-phenyl-1H-pyrazol-5-ol) (3e)

^{1}H NMR (500 MHz, DMSO-d_6): δ 2.33 (6H, s), 4.97 (1H, s) 7.24–7.28 (4H, m), 7.33-7.43 (6H, m), 7.72 (4H, d, *J* = 8.04 Hz), 13.90 (2H, s). ^{13}C NMR (125 MHz, DMSO-d_6, δ/ppm): 12.0, 33.0, 120.9, 121.0, 121.1, 126.0, 126.1, 128.4, 129.3, 129.5, 129.5, 129.5, 129.6, 129.7, 129.8, 131.0, 137.7, 137.7, 137.7, 141.6, 146.7, 146.7.

4,4'-[(4-Methylphenyl) methylene]-bis (3-methyl-1-phenyl-1H-pyrazol-5-ol) (3k)

^{1}H NMR (500 MHz, DMSO-d_6): δ 2.24 (3H, s), 2.32 (6H, s), 4.92 (1H, s), 7.08 (2H, d, *J* = 7.61 Hz), 7.15 (2H, d, *J* = 7.83 Hz), 7.23 (2H, t, *J* = 7.56 Hz), 7.43 (4H, t, *J* = 7.82 Hz), 7.72 (4H, d, *J* = 8.02 Hz), 13.98 (2H, s). ^{13}C NMR (125 MHz, DMSO-d_6,

δ/ppm): 12.1, 20.9, 33.3, 120.9, 121.1, 125.9, 127.5, 129.1, 129.2, 129.3, 129.5, 129.5, 129.5, 129.5, 129.5, 129.6, 135.2, 137.8, 137.8, 139.6, 146.7.

4, 4'-[(4-Benzyloxyphenyl) methylene]-bis (3-methyl-1-phenyl-1H-pyrazol-5-ol) (3m)

^{1}H NMR (500 MHz, DMSO-d_6): *δ* 2.33 (6H, s), 4.92 (1H, s), 5.05 (2H, s), 6.93 (2H, d, *J* = 8.22 Hz), 7.20-7.24 (4H, m), 7.31-7.44 (9H, m), 7.74 (4H, d, *J* = 8.10 Hz), 14.02 (2H, s). ^{13}C NMR (125 MHz, DMSO-d_6, δ/ppm): 12.1, 32.9, 69.6, 114.8, 120.7, 120.8, 120.9, 125.9, 128.0, 128.1, 128.2, 128.5, 128.6, 128.7, 128.8, 129.2, 129.2, 129.3, 134.8, 137.7, 137.8, 137.9, 146.6, 157.1; Mass (EI) m/z: 542.

4, 4'-[(4-Nitrobenzyloxyphenyl) methylene]-bis (3-methyl-1-phenyl-1H-pyrazol-5-ol) (3n)

^{1}H NMR (400 MHz, DMSO-d_6) *δ* 2.25 (s, 6H), 4.86 (s, 1H), 5.17 (s, 2H), 6.87 (d, 2H, *J* = 8.11 Hz), 7.10-7.20 (m, 4H), 7.38 (t, 5H, *J* = 4.05 Hz), 7.63 (t, 5H, *J* = 4.02 Hz), 8.18 (d, 2H, *J* = 4.03 Hz) ppm. ^{13}C NMR (100 MHz, DMSO-d_6, δ/ppm): 11.8, 68.4, 105.5, 114.9, 118.7, 121.4, 124.0, 126.5, 128.5, 128.7, 129.4, 134.8, 137.1, 145.6, 146.5, 147.3, 156.7. Mass (EI) m/z: 587.

Results and Discussion

At first, graphene oxide (GO) was prepared according to the modified Hummers method [41]. IR spectrum of graphene oxide (GO) is appeared in Figure 1a; in which C-O vibration bands can be clearly observed at 1177 cm^{-1}. The vibration of C=O group appeared at 1720 cm^{-1}, while the OH stretching vibration bands can be detected at 3419 cm^{-1}. XRD pattern indicated diffraction peaks in the range of 2Θ=20-30° (Figure 2a). Then, GO (1.00 g) was reacted with 3-aminopyridine (5 mmol) at the presence of *N, N'*-dicyclohexylcarbodiimide (DCC), triethylamine as base and dimethyl acetamide; where dimethyl acetamide served as the solvent, giving rise to the formation of the graphene oxide functionalized pyridine (GO@Py). IR spectrum of (GO@Py) is depicted in Figure 1b; in which C-O vibration bands can be clearly observed at 1024 cm^{-1}. The vibration of C=O group appeared at 1726 cm^{-1}, while the OH stretching vibration bands can be detected at 3422 cm^{-1}. XRD pattern indicated diffraction peaks in the range of 2Θ=20-30° (Figure 2b). Compared to GO XRD pattern (Figure 2a and b), the structure of graphene oxide changed to the structure of graphene.

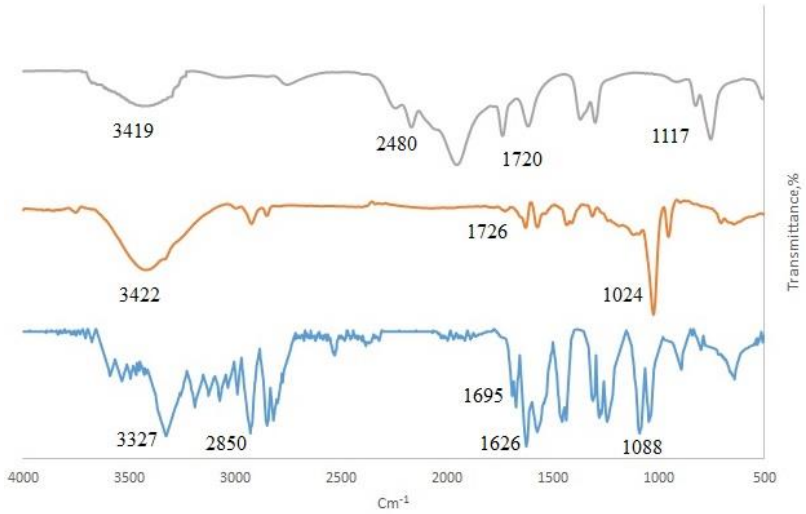

Figure 1. FT-IR spectrum of a) GO, b) GO@Py and c) GO@PyH-CH_3SO_3

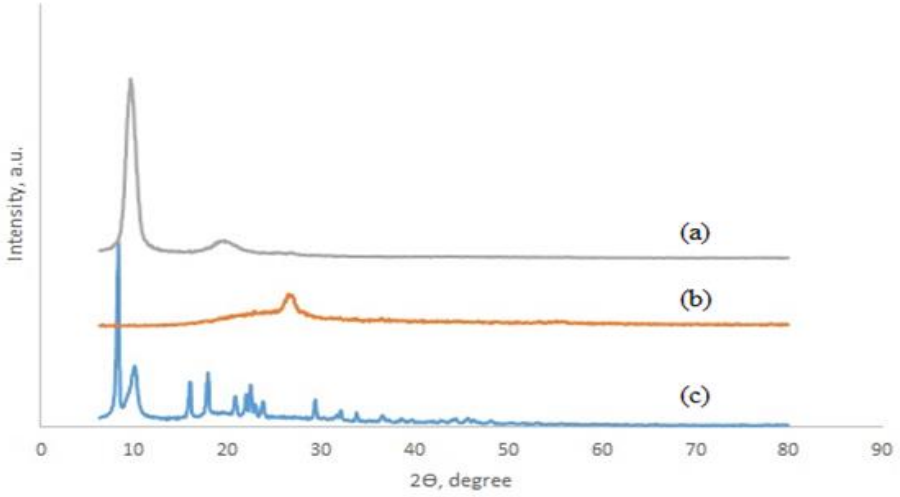

Figure 2. XRD diagram of a) GO, b) GO@Py and c) GO@PyH-CH_3SO_3

Field emission scanning electron microscopy (FESEM) was also utilized to study the morphology of GO@Py (Figure 3). Based on the figure, the structure consisted of tight nano-scaled particles in the size range of 12-45 nm.

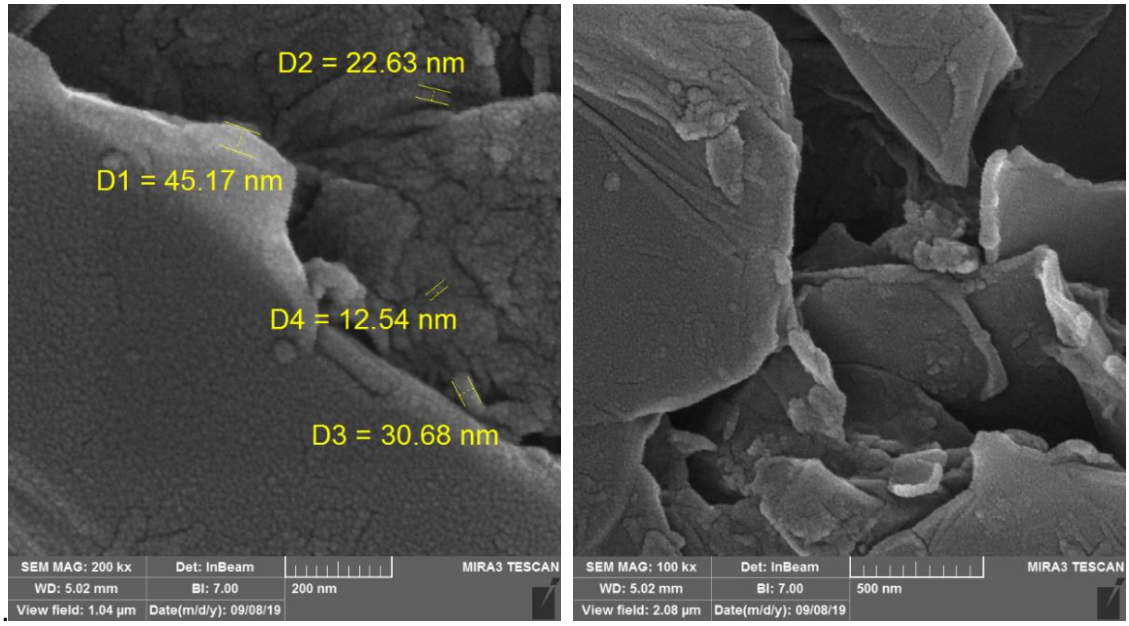

Figure 3. Field emission scanning electron microscopy (FESEM) of graphene oxide functionalized 3-aminopyridine (GO@Py)

According to the energy dispersive spectroscopy (EDS) spectrum of GO@Py (Figure 4), the compound contained no impurities as only the peaks of C, N and O elements were detected. The elemental percentages can be found in the table (Figure 4).

Then, graphene oxide functionalized pyridine-methanesulfonate (GO@PyH-CH_3SO_3) was obtained by treating the GO@Py with

methanesulfonic acid (8 mmol) (Scheme 1). XRD, FT-IR, FESEM, EDX and TGA analysis were employed to characterize the GO@PyH-CH_3SO_3 catalyst.

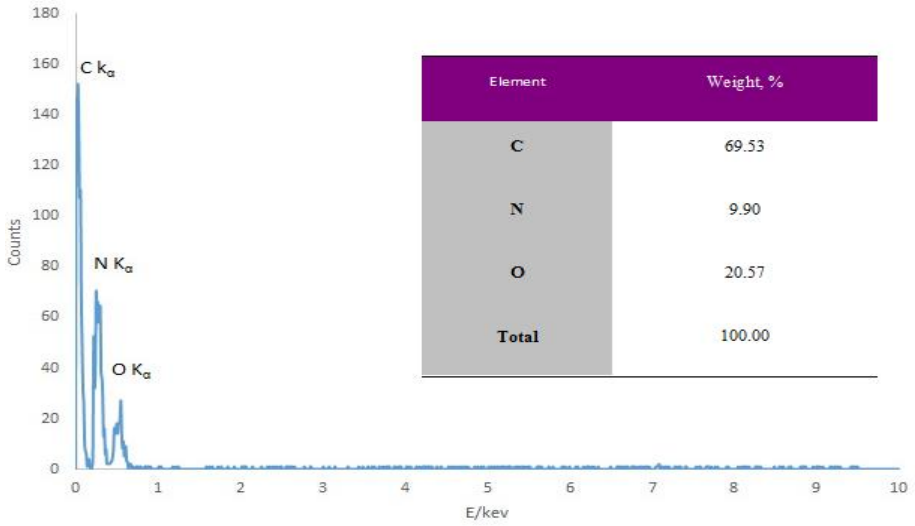

Figure 4. The energy-dispersive X-ray spectroscopy (EDX) diagram and elemental percentages of graphene oxide functionalized 3-aminopyridine (GO@Py)

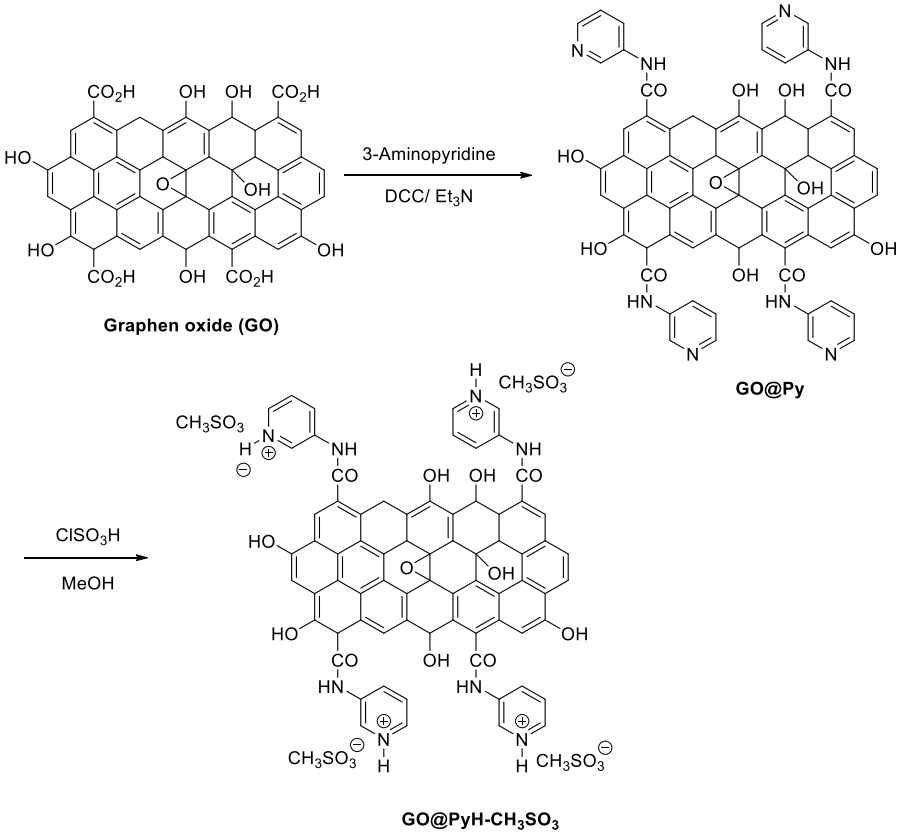

Scheme 1. The synthesis of graphene oxide functionalized 3-aminopyridine (GO@Py) and its methanesulfonate derivative (GO@PyH-CH_3SO_3)

The IR spectrum of the new catalyst is shown in Figure 1c. Stretching vibrations of S–O bond can be found at 892.4 cm^{-1} and 1088.49 cm^{-1}. The band at 1243.9 cm^{-1} can be attributed to the stretching vibrations of C–O bonds; while, the vibrational modes at 1312 cm^{-1} and (2500-3500) cm^{-1} can be assigned to –OH bonds. Also, stretching vibrations. at 1573.9 cm^{-1} and 1626.5 cm^{-1} can be related to C=N and C=O bonds, respectively. Furthermore, C–H and N–H absorption stretching bands can be observed at 3055.5 cm^{-1} and 3327.2 cm^{-1}, respectively. According to the IR spectra appeared in Figure 1, structural changes have been occurred through the synthesis of GO@Py and GO@PyH-CH_3SO_3 from graphene oxide.

As seen in Figure 2, the XRD patterns of GO@PyH-CH_3SO_3 showed diffraction peaks at $2\theta \approx$ 5, 10, 15, 18, 21, 22.5, 24.5 and 29° which confirmed the highly crystalline nature of the catalyst. Thus, according to the Figure 2, GO@PyH-CH_3SO_3 is a highly crystalline compared to GO@Py and graphene oxide.

To explore the thermal stability of GO@PyH-CH_3SO_3, thermogravimetric analysis (TGA) was conducted on the GO@PyH-CH_3SO_3 catalyst as depicted in Figure 5. The weight loss occurred at five steps: (i) 70-160 °C, (ii) 170-230 °C, (iii) 230-280°C (main weight loss), (iv) 280-460°C and (v) 460-560 °C. The first step involved the removal of the adsorbed water. The second weight loss at 170-230 °C can be attributed to the decomposition of substituents on the graphene oxide surface. The third weight loss at 230-280 °C (the main weight loss) can be correlated to the decomposition of the main graphene oxide structure (Figure 5).

Field emission scanning electron microscopy (FESEM) was utilized to study the morphology of GO@PyH-CH_3SO_3 (Figure 6) and show the nanoparticulate structure of the catalyst. The SEM image of the catalyst indicates that the particles were nano-scaled.

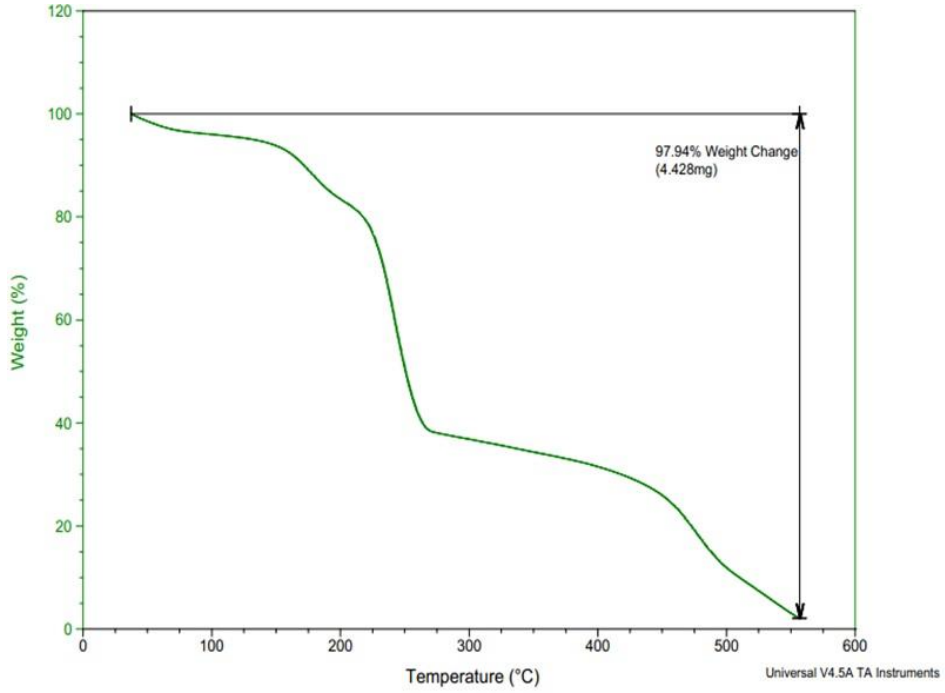

Figure 5. Thermal gravimetric (TG) analysis of graphene oxide functionalized 3-aminopyridine methanesulfonate (GO@PyH-CH_3SO_3)

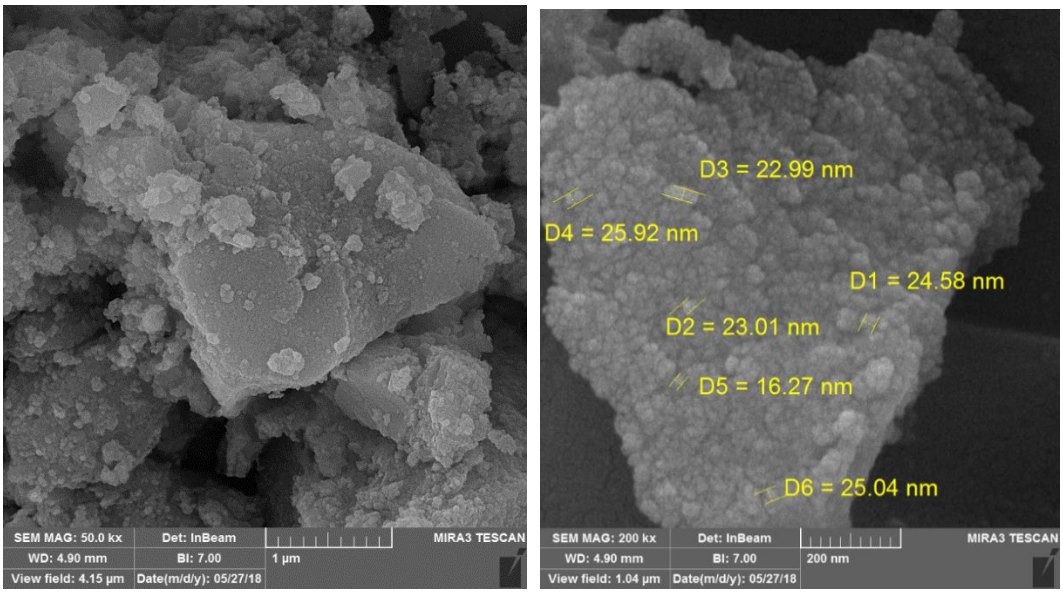

Figure 6. Field emission scanning electron microscopy (FESEM) of graphene oxide functionalized 3-aminopyridine methanesulfonate (GO@PyH-CH_3SO_3)

According to the energy dispersive spectroscopy (EDS) spectrum and elemental percentages of GO@PyH-CH_3SO_3 (Figure 7), the catalyst contained no impurities as only the peaks and weight percents of C, N, O and S elements were detected.

In order to explore the catalytic activity of GO@PyH-CH_3SO_3, the synthesis of pyrazole derivatives were examined. First, the reaction between 3-methyl-1-phenyl-1*H*-pyrazol-5(4*H*)-one and benzaldehyde in the presence of GO@PyH-CH_3SO_3 was optimized (Scheme 2). To this end, 3-methyl-1-phenyl-1*H*-pyrazol-5 (4*H*)-one (2 mmol) and benzaldehyde (1 mmol) (Scheme 2) were reacted at different amounts of GO@PyH-CH_3SO_3 in various solvents and solvent free conditions at the of GO@PyH-CH_3SO_3 catalyst the model reaction (Scheme 2) was performed in the presence of GO, methanesulfonic acid and pyridine methanesulfonate and according to the Table 2, GO@PyH-CH_3SO_3 catalyst has higher yield compared to other catalysts.

Figure 7. The energy-dispersive X-ray spectroscopy (EDX) of graphene oxide functionalized 3-aminopyridine methanesulfonate (GO@PyH-CH_3SO_3)

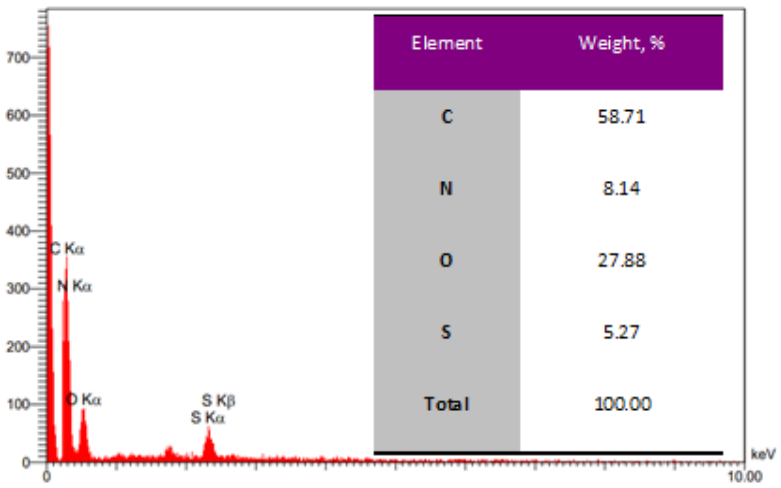

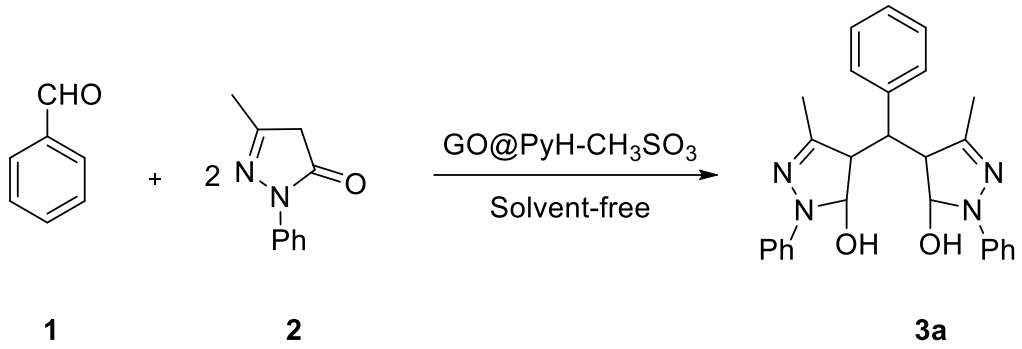

1 **2** **3a**

Scheme 2. The model reaction of the synthesis of 4, 4'-(phenylmethylene)-bis (1*H*-pyrazol-5-ol)s

Table 1. Effect of the catalyst (GO@PyH-CH_3SO_3) quantity, temperature and solvent on the model reaction

Entry	Catalyst amount (g)	Solvent	Temp. (°C)	Time (min)	Yield[a] (%)
1	-	Solvent-free	70	60	34
2	0.01	Solvent-free	70	35	93
3	0.02	Solvent-free	70	10	98
4	0.03	Solvent-free	70	10	98
5	0.02	Solvent-free	60	10	75
6	0.02	Solvent-free	60	40	86
7	0.02	Solvent-free	75	30	94
8	0.02	H_2O	70	90	35
9	0.02	MeCN	70	50	73
10	0.02	Dioxane	70	45	80
11	0.02	$CHCl_3$	Reflux	60	65
12	0.02	$(CH_3)_2CO$	Reflux	60	40
13	0.02	C_2H_5OH	Reflux	20	92
14	0.02	CH_3OH	Reflux	40	87

[a] Isolated yield

Table 2. Effect of catalyst type on the model reaction

Entry	Catalyst[a]	Temp. (°C)	Time (min)	Yield[b] (%)
1	GO	70	10	40
2	CH_3SO_3H	70	10	89
3	Pyridine.CH_3SO_3H	70	10	91
14	GO@PyH-CH_3SO_3	70	10	98

[a] catalyst loading (0.02 g) in solvent-free condition
[b] Isolated yield

To explore the efficiency and the scope of the reaction, several products were synthesized under the optimal conditions using various aryl aldehydes at the presence of GO@PyH-CH_3SO_3 catalyst (Scheme 3, Table 3). As can be seen in Table 3, the reaction was performed at the presence of aryl aldehydes with electron releasing and electron-withdrawing groups as well as halogens on the aromatic ring giving rise to the high product yields.

The structure of product (**3c**) was confirmed by ^{1}H NMR and ^{13}C NMR spectroscopy. Based on ^{1}H NMR results, six methyl protons are observed in 2.34 ppm as a singlet. One methine

proton is observed in 5.15 ppm as a singlet. Two aromatic protons as triplet with *J*=7.62 Hz were observed in 7.25 ppm. Three aromatic protons were also detected as triplet with *J* =7.71 Hz at 7.44 ppm. One aromatic proton is observed as triplet in 7.60 ppm with *J*=8.03 Hz. Moreover, three aromatic protons were observed as doublet with *J*=7.06 Hz in 7.71 ppm. Two aromatic protons were observed as doublet with *J*=13.73 Hz in 8.08 ppm. Two hydroxyl protons were also detected as singlet at 13.90 ppm. Aliphatic and aromatic protons were observed as total of 7 and 14 protons, respectively. Hydroxyl protons were observed as total of 2 protons. Thus according to ^{1}H NMR spectra, the number of protons in the spectra confirmed the structure. ^{13}C NMR spectra showed two aliphatic and 12 aromatic carbons. Thus, ^{13}C NMR confirm the number of carbons. Hence, NMR spectra confirm the structure of **3c.**

The structure of product (**3e**) was confirmed by ^{1}H NMR and ^{13}C NMR spectroscopy. Based on ^{1}H NMR results, six methyl protons are observed in 2.33 ppm as a singlet. One methine proton is observed in 4.97 ppm as a singlet. Four aromatic protons as multiplete were observed in the range of 7.24-7.28 ppm. Six aromatic protons as multiplete were observed in the range of 7.33-7.43 ppm. Four aromatic protons were also detected as doublet with J=8.04 Hz at 7.72 ppm. Two hydroxyl protons were also detected as singlet at 13.90 ppm. Aliphatic and aromatic protons were observed as total of 7 and 14 protons, respectively. Hydroxyl protons were observed as total of 2 protons. Thus according to ^{1}H NMR spectra, the number of protons in the spectra confirmed the structure. ^{13}C NMR spectra shows two aliphatic and 20 aromatic carbons. Thus, ^{13}C NMR confirm the number of carbons. Hence, NMR spectra confirm the structure of **3e.**

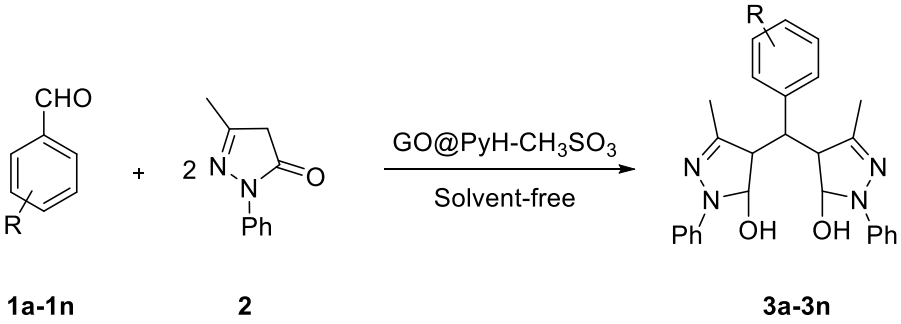

Scheme 3. The synthesis of 4, 4'-(aryl methylene)-bis (1H-pyrazol-5-ol)s catalyzed by GO@PyH-CH_3SO_3

Table 3. The synthesis of 4, 4'-(aryl methylene)-bis (1H-pyrazol-5-ol)s catalyzed by GO@PyH-CH_3SO_3

Comp. no.	Ar	Time (min)	Yield[a] (%)	M.p. (°C)	
				Found	Reported [Lit.]
3a	C_6H_5	20	98	169-170	170-172 [39]
3b	4-$O_2NC_6H_4$	8	98	229-231	230-234 [40]
3c	3-$O_2NC_6H_4$	10	97	150-152	149-150 [36]
3d	2-$O_2NC_6H_4$	12	95	236-237	237-240 [42]
3e	4-ClC_6H_4	10	99	214-216	215-217 [31]

3f	2,4-$Cl_2C_6H_3$	15	97	228-230	227-229 [43]
3g	4-BrC_6H_4	10	97	184-186	183-185 [37]
3h	2-BrC_6H_4	20	95	198-199	198-200 [44]
3i	4-FC_6H_4	12	96	181-182	180-182 [45]
3j	4-$CH_3OC_6H_4$	30	90	174-175	173-175 [43]
3k	4-$CH_3C_6H_4$	20	94	203-205	202-204 [40]
3l	4-OHC_6H_4	30	93	154-155	155-157 [37]
3m	$C_6H_5CH_2OC_6H_4$	30	96	205-207	-
3n	4-NO_2-Ph-CH_2O-p-Ph [46]	30	92	129-130	-

[a] Isolated yield

The structure of product (**3k**) was confirmed by ^{1}H NMR and ^{13}C NMR spectroscopy. Based on ^{1}H NMR results, three methyl protons are observed in 2.24 ppm as a singlet and six methyl protons are observed in 2.32 ppm as a singlet. One methine proton is observed in 4.91 ppm as a singlet. Two aromatic protons as doublet were observed in 7.08 ppm with *J*=7.61 Hz. Two aromatic protons as doublet were observed in 7.15 ppm with *J*=7.83 Hz. Two aromatic protons as doublet were observed in 7.23 ppm with *J*=7.56 Hz. Four aromatic protons as triplet were observed in 7.43 ppm with *J*=7.82 Hz. Four aromatic protons as doublet were observed in 7.72 ppm with *J*=8.02 Hz. Two hydroxyl protons were also detected as singlet at 13.98 ppm. Aliphatic and aromatic protons were observed as total of 10 and 14 protons, respectively. Hydroxyl protons were observed as total of 2 protons. Thus, according to ^{1}H NMR spectra, the number of protons in the spectra confirmed the structure. ^{13}C NMR spectra shows three aliphatic and 18 aromatic carbons. Thus, ^{13}C NMR confirm the number of carbons. Hence, NMR spectra confirm the structure of **3k.**

The structure of product (**3m**) was confirmed by ^{1}H NMR and ^{13}C NMR spectroscopy. Based on ^{1}H NMR results, six methyl protons are observed in 2.33 ppm as a singlet and one methine proton is observed in 4.92 ppm as a singlet. Two methylene protons are observed in 5.05 ppm as a singlet. Two aromatic protons as doublet were observed in 6.93 ppm with *J*=8.22 Hz. Four aromatic protons as multiplete were observed in the range of 7.20-7.24 ppm. Nine aromatic protons as multiplete were observed in the range of 7.31-7.44 ppm. Two hydroxyl protons were also detected as singlet at 14.02 ppm. Aliphatic and aromatic protons were observed as total of 9 and 19 protons, respectively. Hydroxyl protons were observed as total of 2 protons. Thus, according to ^{1}H NMR spectra, the number of protons in the spectra confirmed the structure. ^{13}C NMR spectra showed three aliphatic and 21 aromatic carbons. Thus, ^{13}C NMR confirmed the number of carbons. Hence, NMR spectra confirm the structure of **3m.** Also, mass spectrum confirms the molecular mass of **3m.**

The structure of product (**3n**) was confirmed by ^{1}H NMR and ^{13}C NMR spectroscopy. Based on ^{1}H NMR results, six methyl protons are observed in 2.25 ppm as a singlet and one methine proton is observed in 4.86 ppm as a singlet. Two methylene protons are observed in 5.17 ppm as a singlet. Two aromatic protons as doublet were observed in 6.86 ppm with *J*= 8.11 Hz. Four aromatic protons as multiplete were observed in the range of 7.10-7.20 ppm. Five aromatic protons as triplet were observed in 7.38 ppm with *J*=4.05 Hz. Five aromatic protons as triplet were observed in 7.63 ppm with *J*=4.02 Hz. Two aromatic protons were also detected as doublet in 8.18 ppm with *J*=4.02 Hz. Aliphatic and aromatic protons were observed as total of 9 and 18 protons, respectively. Thus,

according to ^{1}H NMR spectra, the number of protons in the spectra confirmed the structure. ^{13}C NMR spectra revealed three aliphatic and 18 aromatic carbons. Thus, ^{13}C NMR confirmed the number of carbons. Hence, NMR spectra confirm the structure of **3n.** Also, mass spectrum confirms the molecular mass of **3n.**

Mechanism of the reaction for the synthesis of 4, 4'-(aryl methylene)-bis (1*H*-pyrazol-5-ol)s using GO@PyH-CH_3SO_3 nano-catalyst appeared in Scheme 4. According to the mechanism, at first, aldehyde was activated by acidic proton; while 3-methyl-1-phenyl-1*H*-pyrazol-5 (4*H*)-one was activated by methane sulfonate group. Nucleophilic addition of aldehyde and 3-methyl-1-phenyl-1*H*-pyrazol-5 (4*H*)-one followed by water elimination led to benzylidene intermediate (I). Then, Michael addition of second 3-methyl-1-phenyl-1*H*-pyrazol-5 (4*H*)-one molecule to the activated intermediate (I) explored the intermediate (II); by eliminating the second water molecule, the product was obtained (Scheme 4).

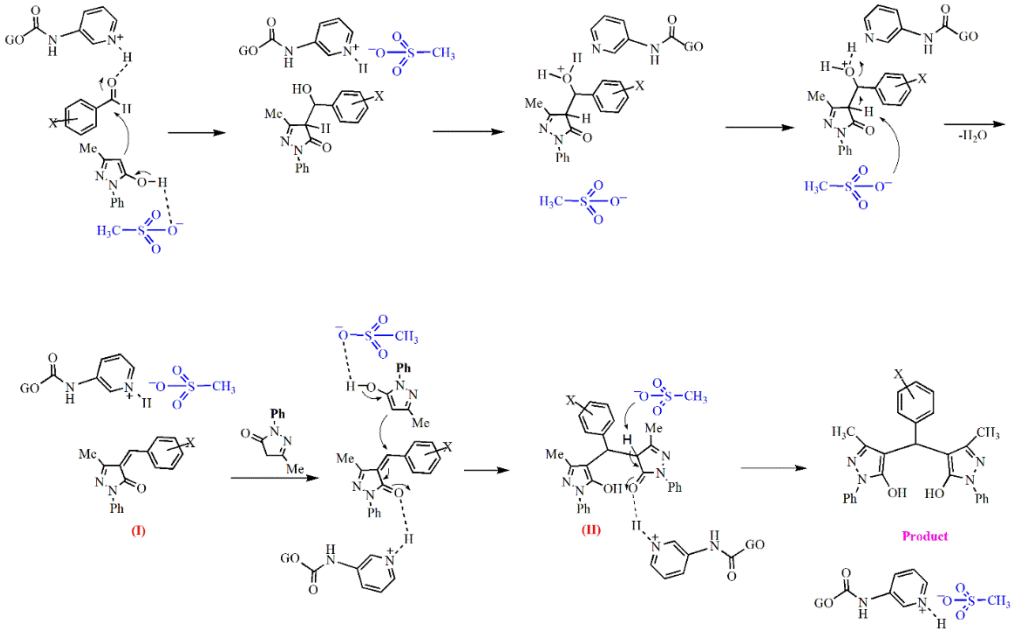

Scheme 4. The proposed mechanism for the preparation of 4, 4'-(aryl methylene)-bis (1*H*-pyrazol-5-ol)s

In order to examine the catalyst in terms of reusability [49-52], it was recovered and then reused for five successive runs. Focusing on the resultant yield of the product (**3a**), no significant change was observed in the yield, confirming the reusability of the catalyst (Figure 8). FT-IR spectra and XRD pattern of GO@PyH-CH_3SO_3 catalyst were reported in Figure 9 and Figure 10 and show no significant change in FT-IR spectrum and XRD pattern. In order to examine the heterogeneous activity of catalyst leaching test were ```` filtered and the catalyst on the filter paper washed with methanol (5 mL). The catalyst was separated on the filter paper and the filtrate were distilled of under reduced pressure. Then, to the flask were added benzaldehyde (**1**, 1mmol, 0.1 mL) and 3-methyl-1-phenyl-1*H*-pyrazol-5 (4*H*)-one (**2**, 2 mmol, 0.34 g) and homogenized and heated at 70 °C for 1 hour with grinding. Then, the mixture was analyzed using TLC and GC and showed the product (**3a**) in 36 percent equal to the catalyst-free percent (Table 2, entry 1).

Thus, this test shows that the catalytic activity was performed at heterogeneous condition.

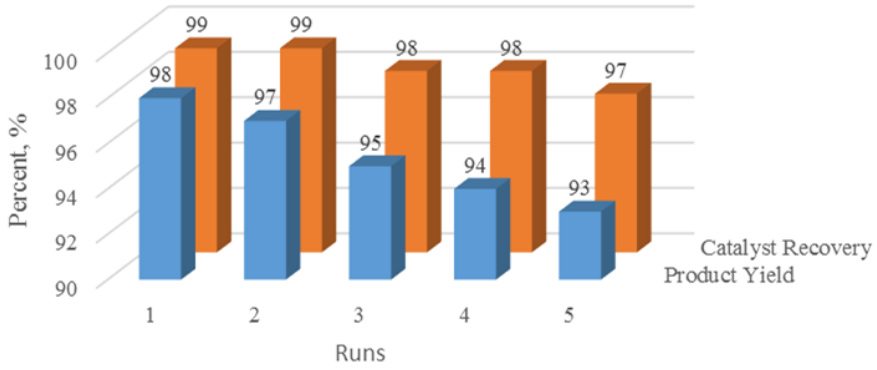

Figure 8. Product yield of **3a** and GO@PyH-CH_3SO_3 catalyst recovery and reusability for five runs

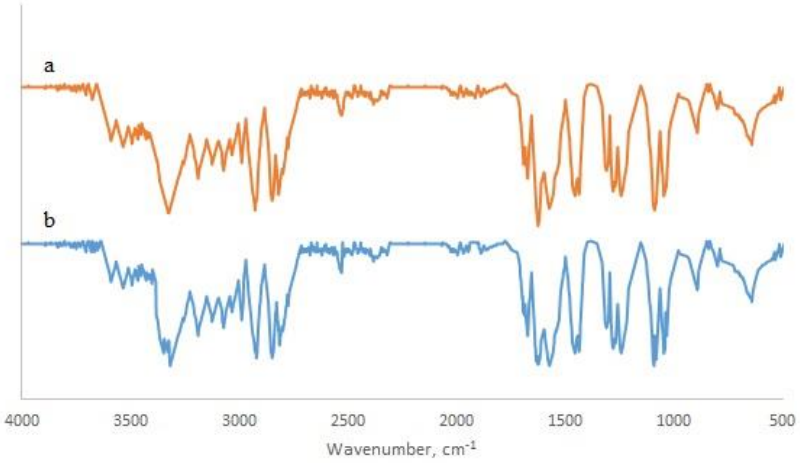

Figure 9. FT-IR spectrum of GO@PyH-CH_3SO_3 catalyst a) before use, b) after recovery

Figure 10. XRD diagram of GO@PyH-CH_3SO_3 catalyst a) before use, b) after recovery

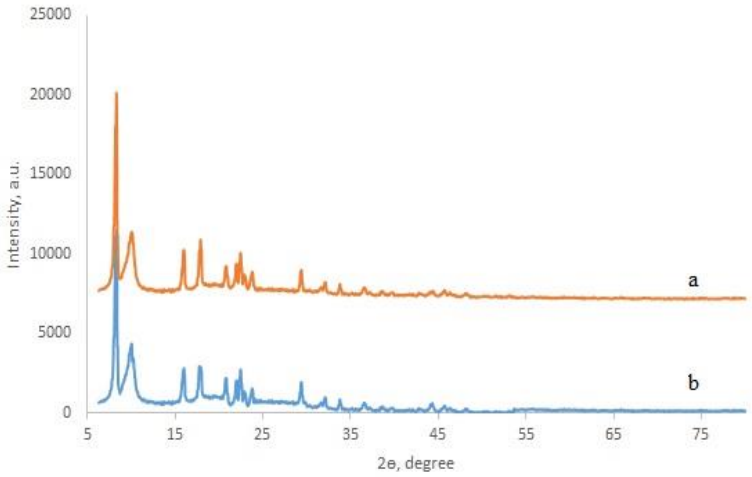

Efficiency and capability of the GO@PyH-CH_3SO_3 catalyst and other catalysts in the synthesis of bis pyrazolines were compared (Table 4). As shown in Table 4, GO@PyH-CH_3SO_3 has the higher yield and improved green reaction condition compared to other catalysts.

Table 4. Comparison of the results on the synthesis of 4, 4'-(phenylmethylene)bis (*3-methyl-1-phenyl-2-pyrazoline-5-one*) (**3a**) catalyzed by GO@PyH-CH_3SO_3 with those obtained by the other catalyst [a]

Entry	Catalyst (mg)	Solvent	Temperature, (°C)	Time (Min.)	Yield [b] (%) [Ref.]
1	GO@PyH-CH_3SO_3 (20)	Solvent Free	70	10	98 [This work]
2	1,10-PHTNM (10)	H_2O	80	20	95 [47]
3	ZnO nanoparticles (2 mol%)	EtOH,H_2O	Reflux	20	92 [48]
4	SBS-Sulfonic acid (100)	EtOH	Reflux	120	80 [25]
5	Cellulose sulfuric acid (20)	EtOH, H_2O	Reflux	120	74 [31]
6	SBNPTT (30)	EtOH	Reflux	30	90 [44]
7	PEG-SO3H (1.5 mol %)	H_2O	Reflux	30	92 [26]
8	Xanthan sulfuric acid (80)	EtOH	Reflux	15	95 [40]

[a] The reactions were carried out by the condensation of *3-methyl-1-phenyl-2-pyrazoline-5-one* with benzaldehyde
[b] Isolated yield

Conclusions

Graphene oxide functionalized 3-amino pyridine can be prepared from graphene oxide and 3-aminopyridine (GO@Py). GO@PyH-CH_3SO_3 nano-catalyst can be afforded from the reaction of GO@Py and methanesulfonic acid. The efficient synthesis of the 4, 4'-(aryl methylene)-bis (1H-pyrazol-5-ol) derivatives from aryl aldehydes and 3-methyl-1-phenyl-1*H*-pyrazol-5 (4*H*)-one could be achieved at the presence of the GO@PyH-CH_3SO_3 nanocatalyst. The use of graphene-based nano-catalyst (as an inexpensive, easily-synthesized nano-catalyst) revealed several advantages including, among which, nontoxicity, generality, short reaction times, simple work-up and mild reaction conditions can be mentioned. In addition, the simple recovery and reusability of catalyst and no significant change in recovery and product yield showed the capability of catalyst. The leaching test demonstrated the heterogeneous activity of catalyst. Efficiently and capability of GO@PyH-CH_3SO_3 catalyst and other catalysts were compared and showed the superior properties of this catalyst.

Acknowledgments

The authors would like to appreciate the Payame Noor University (PNU) Research Council for supporting this research study.

Disclosure Statement

No potential conflict of interest was reported by the authors.

Orcid

Esmael Rostami 0000-0002-6512-9951

References

[1]. Rogers B., Adams J., Pennathur S., *Nanotechnology: understanding small systems*. CRC Press, 2014
[2]. Amin P., Patel M. *Asian J. Nanosc. Mater.,* 2020, **3**:24
[3]. Chen M.N., Mo L.P., Cui Z.S., Zhang Z.H. *Curr. Opin. Green Sustain. Chem.*, 2019, **15**:27
[4]. Lui C.H., Liu L., Mak K.F., Flynn G.W., Heinz T.F. *Nature*, 2009, **462**:339
[5]. Akinwande D., Brennan C.J., Bunch J.S., Egberts P., Felts J.R., Gao H., Huang R., Kim J.S., Li T., Li Y., Liechti K.M. *Extreme Mech. Lett.*, 2017, **13**:42
[6]. Rabiee N., Safarkhani M., Rabiee M. *Asian J. Nanosc. Mater.,* 2018, **1**:63
[7]. Zhu Y., Murali S., Cai W., Li X., Suk J.W., Potts J.R., Ruoff R.S. *Adv. Mater.*, 2010, **22**:3906
[8]. Rambabu G., Bhat S.D. *J. Membrane Sci.*, 2018, **551**:1
[9]. Ahmad H., Fan M., Hui D. *Compos. Part B: Eng.*, 2018, **145**:270
[10]. Küçükgüzel Ş.G., Şenkardeş S. *Eur. J. Med. Chem.*, 2015, **97**:786
[11]. Kumar V., Kaur K., Gupta G.K., Sharma A. K. *Eur. J. Med. Chem.*, 2013, **69**:735
[12]. Magda A.A., Abdel-Aziz N.I., Alaa El-Azab A. M.A.S., Asiri Y.A., El Tahir K.E. *Bioorgan. Med. Chem.*, 2011**, 19**:3416
[13]. Mohamed L.W., Shaaban M.A., Zaher A.F., Alhamaky S.M., Elsahar A.M. *Bioorg. Chem.*, 2019, **83**:47
[14]. Bhavanarushi S., Kanakaiah V., Bharath G., Gangagnirao A., Rani J.V. *Med. Chem. Res.*, 2014, **23**:158
[15]. Rosiere C.E., Grossman M.I. *Science*, 1951, **113**:651
[16]. Bailey D.M., Hansen P.E., Hlavac A.G., Baizman E.R., Pearl J., De Felice A.F., Feigenson M.E. *J. Med. Chem.*, 1985, **28**:256
[17]. do Carmo Malvar D., Ferreira R.T., de Castro R.A., de Castro L.L., Freitas A.C.C., Costa E. A., Florentino I.F., Mafra J.C.M., de Souza G.E.P., Vanderlinde F.A. *Life Sci.*, 2014, **95**:81
[18]. Sugiura S., Ohno S., Ohtani O., Izumi K., Kitamikado T., Asai H., Kato K., Hori M., Fujimura H. *J. Med. Chem.*, 1977, **20**:80
[19]. Pitucha M., Mazur L., Kosikowska U., Pachuta-Stec A., Malm A., Popiołek Ł., Rzączyńska Z. *Heteroatom Chem.*, 2010**, 21**:215
[20]. Lubs H.A. The Chemistry of Synthetic Dyes and Pigments, Ed.; American Chemical Society: Washington, DC, 1970
[21]. Londershausen M. *Pestic. Sci.*, 1996, **48**:269
[22]. Singh D., Singh D. J., *Indian Chem.* Soc., 1991, **68**:165
[23]. Sridhar R., Perumal P.T., Etti S., Shanmugam G., Ponnuswamy M.N., Prabavathy V. R., Mathivanan N. *Bioorg. Med. Chem. Lett.*, 2004, **14**:6035
[24]. Sivaprasad G., Perumal P.T., Prabavathy V. R., Mathivanan N. *Bioorg. Med. Chem. Lett.*, 2006, **16**:6302
[25]. Niknam K., Saberi D., Sadegheyan M., Deris A. *Tetrahedron Lett.*, 2010, **51**:692
[26]. Hasaninejad A., Shekouhy M., Zare A., Ghattali S.H., Golzar N. *J. Iran. Chem. Soc.*, 2011, **8**:411
[27]. Niknam K., Mirzaee S. *Synth. Commun.*, 2011, **41**:2403
[28]. Sujatha K., Shanthi G., Selvam N. P., Manoharan S., Perumal P. T., Rajendran M. *Bioorg. Med. Chem. Lett.*, 2009, **19**:4501
[29]. Sobhani S., Safaei E., Hasaninejad A.R., Rezazadeh S. *J. Organomet. Chem.*, 2009, **694**:3027
[30]. Gouda M.A., Abu-Hashem A.A. *Green Chem. Lett. Rev.*, 2012, **5**:203
[31]. Tayebi S., Baghernejad M., Saberi D., Niknam K. *Chinese J. Catal.*, 2011, **32**:1477
[32]. Khazaei A., Zolfigol M.A., Moosavi-Zare A. R., Asgari Z., Shekouhy M., Zare A. Hasaninejad A. *RSC Adv.*, 2012, **2**:8010
[33]. Sobhani S., Hasaninejad A.R., Maleki M.F., Parizi Z.P. *Synth. Commun.*, 2012**, 42**:2245

[34]. Phatangare K.R., Padalkar V.S., Gupta V.D., Patil V.S., Umape P.G., Sekar N. *Synth. Commun.*, 2012, **42**:1349
[35]. Baghernejad M., Niknam K. *Int. J. Chem.*, 2012, **4**:52
[36]. Wang W., Wang S.X., Qin X.Y., Li J.T. *Synth. Commun.*, 2005, **35**:1263
[37]. Karimi-Jaberi Z., Pooladian B., Moradi M., Ghasemi E. *Chinese J. Catal*., 2012, **33**:1945
[38]. Sobhani S., Nasseri R., Honarmand M. *Can. J. Chem.*, 2012**, 90**:798
[39]. Mosaddegh E., Hassankhani A., Baghizadeh A. *J. Chil. Chem. Soc.*, 2010, **55**:419
[40]. Kuarm B.S., Rajitha B. *Synth. Commun.*, 2012, **42**:2382
[41]. Yu H., Zhang B., Bulin C., Li R., Xing R. *Sci. Rep.*, 2016, **6**:36143
[42]. *Zhoui* Z., *Zhang Y.* J. *Chil. Chem. Soc.*, 2015, **60**:2992
[43]. Iravani N., Albadi J., Momtazan H., Baghernejad M. *J. Chin. Chem. Soc.*, 2013, **60**:418
[44]. Soleimani E., Ghorbani S., Taran M., Sarvary A. *C. R. Chim.*, 2012, **15**:955
[45]. Niknam K., Habibabad M. S., Deris A., Aeinjamshid N. *Monatsh. Chem.*, 2013**, 144**:987
[46]. Rostami E., Zare S. H. *ChemistrySelect,* 2019**, 4**:13295
[47]. Dashteh M., Baghery S., Zolfigol M.A., Bayat Y., Asgari A. *ChemistrySelect*, 2019, **4**:337
[48]. Eskandari K., Karami B., Khodabakhshi S. *Chem. Heterocycl. Compd.*, 2015, **50:**1658
[49]. Alinezhad H., Tarahomi M., Maleki B. and Amiri A. *Appl. Organomet. Chem.*, 2019, **33**:e4661
[50]. Baghayeri M., Alinezhad H., Tarahomi M., Fayazi M., Ghanei-Motlagh M., Maleki B. *Appl. Surf. Sci.*, 2019, **478**:87
[51]. Tarahomi M., Alinezhad H., Maleki B. *Appl. Organomet. Chem.*, 2019, **33**:e5203
[52]. Baghayeri M., Alinezhad H., Fayazi M., Tarahomi M., Ghanei-Motlagh R., Maleki B. *Electrochimica Acta*, 2019, **312**:80

How to cite this manuscript: Esmael Rostami*, Zahra Kordrostami. An efficient synthesis of 4, 4'-(aryl methylene)-bis (1*H*-pyrazol-5-ol)s over graphene oxide Functionalized pyridine-methanesulfonate as a novel nanocatalyst. *Journal of Medicinal and Nanomaterials Chemistry*, 2(3) 2020, 203-219. DOI: 10.48309/JMNC.2020.3.4